



## Structural Performance of Triangular Latticed Shells with Regularized Panels for Bézier Design Surfaces

Kazuki HAYASHI\*, Makoto OHSAKI <sup>a</sup>

\* Department of Architecture and Architectural Engineering, Graduate School of Engineering, Kyoto University  
Kyoto-Daigaku Katsura, Nishikyo, Kyoto 615-8540, Japan  
E-mail: [hayashi.kazuki.55a@st.kyoto-u.ac.jp](mailto:hayashi.kazuki.55a@st.kyoto-u.ac.jp)

<sup>a</sup> Department of Architecture and Architectural Engineering, Graduate School of Engineering, Kyoto University

### Abstract

We propose a new method for regularization of triangular latticed shell panels whose design surface is a tensor product Bézier surface. The planar triangular panels are classified into clusters using the data set consisting of three edge lengths of each triangle. In this clustering, a continuous participation function is introduced instead of discretized one for representing degree of contribution to the clusters. Furthermore, by solving an optimization problem to minimize the difference between the maximum and minimum lengths, more uniform panel shapes can be obtained within every cluster. We further carry out structural analysis on the initial and the optimal solutions to compare their structural performance.

**Keywords:** latticed shell, tensor product Bézier surface, regularization, structural optimization, clustering, panelization.

### 1. Introduction

Recently, free-form surfaces are utilized as design surfaces for roof structures. Accordingly, there is an increasing interest in obtaining rational shapes considering cost and constructability of free-form surfaces. Discretization to latticed shell is an effective way to reduce cost, and uniformity of discretized members is a key factor for this purpose because it can contribute to reduce the number of types of members and joints. Moreover, regularization of members is expected to prevent buckling of extremely long members and difficulty in constructability due to short members.

Ohsaki and Fujita [1] proposed a geometry optimization method for minimizing strain energy and variance of member length. However, this method does not necessarily yield solutions with less difference of member lengths. Ogawa et al. [2] used the difference between the maximum and minimum lengths for the regularization of member lengths.

As an extension of the method for uniform member lengths, uniform triangular planar panel shapes can be achieved by using the data set consisting of the three edge lengths of each panel. Singh and Schaefer [3] proposed a regularization method for a mesh of triangles, where initial triangles are classified by k-means clustering and the vertices are relocated by solving an optimization problem so that the surface polygons match the canonical polygons as close as possible. However, this method inevitably alters the geometry of surface and may cause an unexpected change of structural behavior.

Hayashi and Ohsaki [4] presented a regularization method to obtain uniform triangular panels within several groups. The design variables are parameters defining the locations of the nodes on a prescribed tensor product Bézier surface, and the nodes strictly move on the surface during the optimization without

any gap between the panels. In the process of clustering, continuous values are introduced to express the degree of participation to each cluster for panel shapes. However, Euclidean distance of three edge lengths is used in the process of clustering and optimization, which is not necessarily effective to minimize the difference of edge lengths.

In this paper, we introduce a Minkowski distance ( $p$ -norm) instead of Euclidean distance for expressing the degree of participation and objective function. By applying large value for  $p$ , the order of the distance, almost the same effect as minimization of the largest discrepancy in edge lengths can be achieved, while conserving the continuity of the objective function. Effectiveness of the proposed method is demonstrated in the numerical examples of two design surfaces; one with large curvature and the other with the half scale in the height direction.

Furthermore, we compare structural performance of these examples by means of FEM analysis, and quantitatively evaluate the trade-off between the degree of difficulty in regularization and structural performance of latticed shells in terms of the curvature of the design surface.

## 2. Regularization of panel shapes

The overall workflow of the regularization method is described in this section. Discretization of tensor product Bézier surface is explained, and two fundamental procedures, clustering and optimization, are formulated.

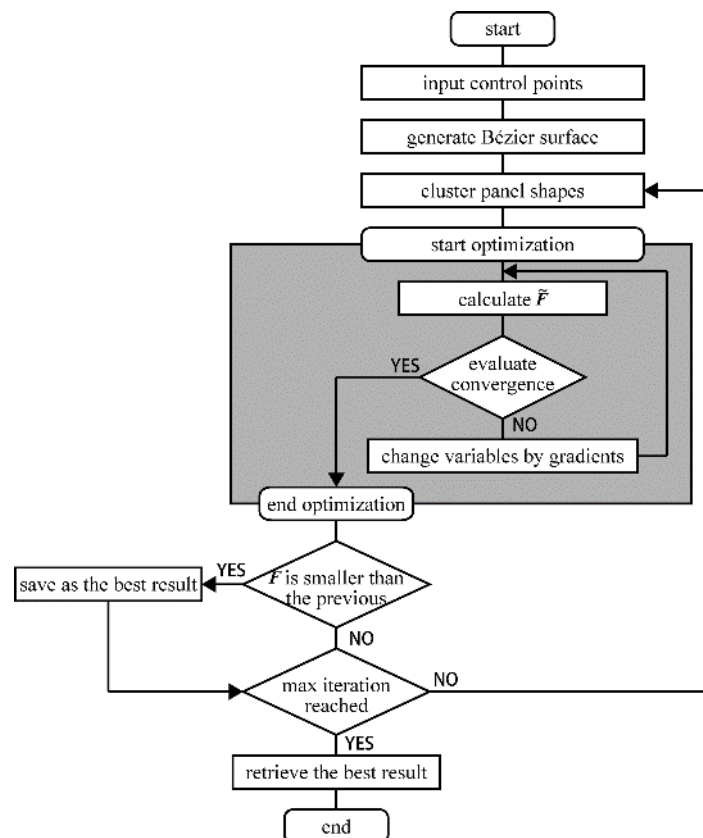


Figure 37: Overall workflow of the regularization process.

## 2.1. Panel generation from tensor product Bézier surface

In general, a tensor product Bézier surface of order  $M \times N$  is expressed with parameters  $u, v \in [0, 1]$  as

$$\mathbf{S}(u, v) = \sum_{i=0}^M \sum_{j=0}^N B_i^M(u) B_j^N(v) \mathbf{R}_{ij} \quad (1a)$$

$$B_i^M(u) = \binom{M}{i} u^{M-i} (1-u)^i \quad (1b)$$

$$B_j^N(v) = \binom{N}{j} v^{N-j} (1-v)^j \quad (1c)$$

where  $B_i^M(u)$  and  $B_j^N(v)$  are the Bernstein basis polynomials, and  $\mathbf{R}_{ij} \in \mathbb{R}^3$  is a position vector of  $(i, j)$  control point. Note that the locations of control points are all fixed in this paper, that is,  $\mathbf{R}_{ij}$  is constant for  $i=0, \dots, M$  and  $j=0, \dots, N$ .

Next, finite number of nodes are generated on the surface by assigning the parameter sets  $(u_k, v_k)$  of each node into equation (1). The neighboring nodes are connected to create a triangular mesh. Therefore, if the connectivity is fixed, nodal locations of the panel can be described as a function of  $(u_k, v_k)$ .

## 2.2. Clustering

The  $n_d$  triangular meshes are classified into  $n_c$  groups. To apply this clustering method to triangular panels, three edge lengths of each triangular panel  $\mathbf{x}_i = \{L_{i,1}, L_{i,2}, L_{i,3}\}$  ( $L_{i,1} \leq L_{i,2} \leq L_{i,3}$ ) are computed. The initial locations of cluster centroids are chosen to avoid their proximity as follows; one of the data  $\mathbf{x}_i$  ( $i=1, \dots, n_d$ ) is randomly chosen as the first centroid, and the other centroids are chosen from data according to the probability [5,6]:

$$p(\mathbf{x}_i) = \frac{D(\mathbf{x}_i)^2}{\sum_{i=1}^{n_d} D(\mathbf{x}_i)^2} \quad (2)$$

where  $D(\mathbf{x}_i)$  is an euclidian distance from  $\mathbf{x}_i$  to the closest centroid.

After obtaining the initial cluster centroids  $\mathbf{c}_j = \{\bar{L}_{j,1}, \bar{L}_{j,2}, \bar{L}_{j,3}\}$  ( $\bar{L}_{j,1} \leq \bar{L}_{j,2} \leq \bar{L}_{j,3}$ ), clustering is conducted. The degree of participation in cluster  $j$  for data  $i$  is computed as

$$U_{ij} = \left( \sum_{k=1}^c \left( \frac{\|\mathbf{x}_i - \mathbf{c}_k\|_p}{\|\mathbf{x}_i - \mathbf{c}_j\|_p} \right)^{\frac{2}{m-1}} \right)^{-1} \quad (i=1, \dots, n_d, j=1, \dots, n_c) \quad (3)$$

where  $m$  is a clustering parameter; if  $m$  is sufficiently large, degree of participation of data  $i$  becomes almost equal for all the clusters. Note that Minkowski distance with order  $p$  is applied to equation (3).

As  $p$  takes larger value,  $\|\mathbf{x}_i - \mathbf{c}_j\|_p$  becomes the largest difference among three edge lengths, expressed as

$$\lim_{p \rightarrow \infty} \|\mathbf{x}_i - \mathbf{c}_j\|_p = \max_{k=1,2,3} (L_{i,k} - \bar{L}_{j,k}) \quad (4)$$

In view of trade-off between accuracy of the maximum value and smoothness of the function, the order  $p$  is set to be 10 in this research.

Regarding  $U_{ij}$  as weight coefficient, the cluster centroids are updated as

$$\mathbf{c}_j = \frac{\sum_{i=1}^{n_d} U_{ij}^m \mathbf{x}_i}{\sum_{i=1}^{n_d} U_{ij}^m} \quad (5)$$

Equations (3) and (5) are alternately computed until the values of  $U_{ij}$  converge. In distributing data to the clusters, we choose the cluster with the maximum degree of participation among all the clusters.

### 2.3. Optimization

The aim of the optimization is to minimize the difference of maximum and minimum edge lengths of the panel within every cluster, expressed as

$$F(\mathbf{u}, \mathbf{v}) = \max_j \left( \max_{i_1, i_2} \left( \max_{k=1,2,3} \|L_{i_1, k}^j - L_{i_2, k}^j\| \right) \right) \quad (6)$$

where  $L_{i_1, k}^j$  and  $L_{i_2, k}^j$  are the  $k$ th edge of  $i_1$ th and  $i_2$ th panel in cluster  $j$ , and  $\mathbf{u}$  and  $\mathbf{v}$  are the vectors of all variables  $u_k$  and  $v_k$ , respectively. We modify the objective function to improve the differentiability, and assign the admissible regions  $\Omega_{\mathbf{u}}$  and  $\Omega_{\mathbf{v}}$  for  $\mathbf{u}$  and  $\mathbf{v}$  to formulate the optimization problem as

$$\text{minimize } \tilde{F}(\mathbf{u}, \mathbf{v}) = \max_j \left( \max_{i_1, i_2} \|\mathbf{x}_{i_1}^j - \mathbf{x}_{i_2}^j\|_{10} \right) \quad (7a)$$

$$\text{subject to } \mathbf{u} \in \Omega_{\mathbf{u}} \quad (7b)$$

$$\mathbf{v} \in \Omega_{\mathbf{v}} \quad (7c)$$

where  $\mathbf{x}_{i_1}^j$  and  $\mathbf{x}_{i_2}^j$  are the  $i_1$ th and  $i_2$ th data in cluster  $j$ .  $\max_{i_1, i_2} \|\mathbf{x}_{i_1}^j - \mathbf{x}_{i_2}^j\|_{10}$  is the maximum value of the Minkowski distance with order 10 of three edge lengths within cluster  $j$ , and it is computed for every cluster to extract the maximum value, which becomes the objective function  $\tilde{F}$ .

Note that clustering and optimization are alternately and iteratively conducted for 100 times, respectively. After each iteration, we substitute the optimal design variables for equation (6), and preserve the best solution with the least value  $\tilde{F}$ . We retrieve the best solution after 100 iterations and set it as an output.

## 2.4. Sensitivity analysis

In solving the optimization problem (7), we use a sequential quadratic programming, which is a gradient-based approach of nonlinear programming. Therefore, sensitivity coefficients of objective function are necessary to reduce computation time.

Let  $\tilde{F}_e$  denote the Minkowski distance with order 10 between  $i_1$  th and  $i_2$  th panels, which is written as

$$\begin{aligned}\tilde{F}_e &= \|\mathbf{x}_{i_1} - \mathbf{x}_{i_2}\|_{10} \\ &= \left( \sum_{k=1}^3 (L_{i_2,k} - L_{i_1,k})^{10} \right)^{\frac{1}{10}}\end{aligned}\quad (8)$$

Differentiation of  $\tilde{F}_e = \|\mathbf{x}_{i_1} - \mathbf{x}_{i_2}\|_{10}$  with respect to  $u_l$  leads to

$$\frac{\partial \tilde{F}_e}{\partial u_l} = \frac{1}{10} \cdot \left( \sum_{k=1}^3 (L_{i_2,k} - L_{i_1,k})^{10} \right)^{-\frac{9}{10}} \cdot 10 \cdot \sum_{k=1}^3 \left( (L_{i_2,k} - L_{i_1,k})^9 \cdot \left( \frac{\partial L_{i_2,k}}{\partial u_l} - \frac{\partial L_{i_1,k}}{\partial u_l} \right) \right) \quad (9)$$

Sensitivity coefficient of  $L_{i,k}$  with respect to  $u_l$  is obtained as

$$\frac{\partial L_{i,k}}{\partial u} = \frac{\partial \|\mathbf{p}_{i,k}^e - \mathbf{p}_{i,k}^s\|}{\partial u} \quad (10)$$

where  $\mathbf{p}_{i,k}^s$  and  $\mathbf{p}_{i,k}^e$  are the locations of the start and end points of  $k$  th edge of the  $i$  th panel, which can be derived from equation (1a). Sensitivity coefficient of  $\mathbf{S}(u_l, v_l)$  in (1a) with respect to  $u_l$  is given by

$$\frac{\partial \mathbf{S}(u_l, v_l)}{\partial u_l} = \sum_{i=0}^M \sum_{j=0}^N \frac{\partial B_i^M(u_l)}{\partial u_l} B_j^N(v) \mathbf{R}_{ij} \quad (11)$$

Differentiation of (1b) with respect to Sensitivity coefficient of Bernstein polynomials leads to

$$\frac{\partial B_i^M(u_l)}{\partial u_l} = \binom{M}{i} \left( (M-i) \cdot u_l^{M-i-1} (1-u_l)^i - i \cdot u_l^{M-i} (1-u_l)^{i-1} \right) \quad (12)$$

By backpropagating computations from (12) to (9), gradients of the objective function with respect to  $\mathbf{u}$  can be analytically calculated, and that with regard to  $\mathbf{v}$  can be derived in a similar way.

## 4. Numerical examples

Examples of two design surfaces are demonstrated in this section within the framework of Python 3.6.4 and SLSQP [7] to solve the optimization problem. Units for nodal coordinates and edge lengths are expressed in meters, and their representations are omitted in the following examples. The number of clusters is set to be ten and clustering parameter  $m$  is 2.0.

In the latter part of this section, structural analysis is conducted for the examples to understand the relationship between the degree of difficulty in the regularization and structural performance of the latticed shells from the perspective of curvature of the design surface.

#### 4.1. Example 1: surface with large curvature

The control polygon is composed of 25 points, as listed in Table 1, to create a quartic tensor product Bézier surface as shown in the left Fig. 2. The number of equal mesh division is ten in  $u$  and  $v$  directions. Connecting neighboring nodes generates an initial shape with 121 nodes and 200 triangular panels as shown in the right Fig. 2. Average lengths of long, middle, and short sides are 1.695, 1.206, and 1.052, respectively.

Table 2: Numbering of control points (colored in gray) and their coordinates.

1	(-5.0, -5.0, 3.0)	6	(-2.5, -5.0, 1.5)	11	(0.0, -5.0, 0.0)	16	(2.5, -5.0, -1.5)	21	(5.0, -5.0, -3.0)
2	(-5.0, -2.5, 1.5)	7	(-2.5, -2.5, 5.0)	12	(0.0, -2.5, -5.0)	17	(2.5, -2.5, -5.0)	22	(5.0, -2.5, -1.5)
3	(-5.0, 0.0, 0.0)	8	(-2.5, 0.0, 2.0)	13	(0.0, 0.0, 5.0)	18	(2.5, 0.0, 5.0)	23	(5.0, 0.0, 0.0)
4	(-5.0, 2.5, -1.5)	9	(-2.5, 2.5, -5.0)	14	(0.0, 2.5, -5.0)	19	(2.5, 2.5, -5.0)	24	(5.0, 2.5, 1.5)
5	(-5.0, 5.0, -3.0)	10	(-2.5, 5.0, -1.5)	15	(0.0, 5.0, 0.0)	20	(2.5, 5.0, 1.5)	25	(5.0, 5.0, 3.0)

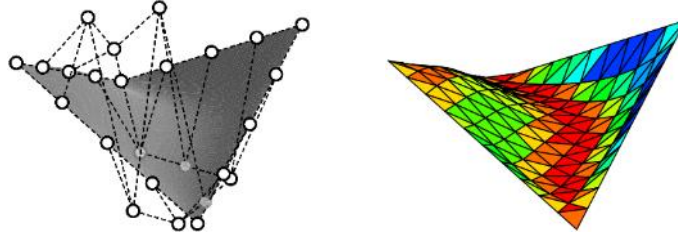


Figure 38: Control polygon of tensor product Bézier surface (left) and its initial panelization (right).

$\Omega_u$  is set such that the parameter  $u_k$  simultaneously satisfy  $u_k \in [0, 1]$  and  $u_k \in [\bar{u}_k - 0.09, \bar{u}_k + 0.09]$ , where  $\bar{u}_k$  is an initial value of  $u_k$ .  $\Omega_v$  is set in the same way. As for mesh vertices on the edges of the surface, We further add constraint for  $u_k$  or  $v_k$  on an edge such that it keeps moving on the edge; accordingly, four corner nodes cannot move in the optimization.

The iteration history of objective value computed by equation (6) is described in Fig. 3. The improvement of  $F$  is remarkable especially in the early stage of iterations. The best regularization solution is retrieved from 31st iteration and its result is described in Table 2.  $N'$  is the number of panels belonging to the cluster, and  $L_l^U - L_l^L$ ,  $L_m^U - L_m^L$ , and  $L_s^U - L_s^L$  are the maximum differences of long, middle, and short sides of triangular panels within the same cluster, respectively. Since the largest difference has decreased from 0.212 to 0.096, more uniform triangular panels are obtained. As the right of Table 2 shows, regularized panels contain almost the same value in maximum discrepancy of edge lengths within every cluster, within the range of 0.073 and 0.096. These observations imply that the objective function (7a) using Minkowski distance efficiently works to minimize (6): our original intention for the regularization.

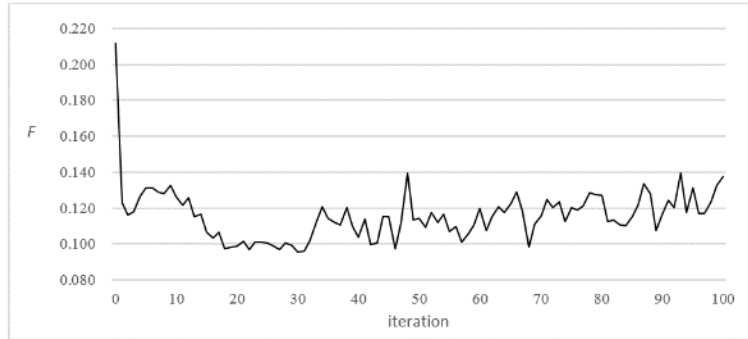


Figure 39: Iteration history of objective value  $F$ .

Table 3: Regularization result.

cluster	Initial panelization				Regularized panelization			
	$N^i$	$L_i^U - L_i^L$	$L_m^U - L_m^L$	$L_s^U - L_s^L$	$N^i$	$L_i^U - L_i^L$	$L_m^U - L_m^L$	$L_s^U - L_s^L$
0	32	0.024	0.080	0.045	24	0.092	0.089	0.096
1	43	0.166	0.130	0.176	24	0.080	0.091	0.092
2	36	0.047	0.140	0.156	30	0.091	0.096	0.093
3	26	0.086	0.129	0.149	44	0.095	0.096	0.095
4	21	0.047	0.089	0.145	27	0.086	0.095	0.096
5	11	0.116	0.146	0.122	16	0.095	0.095	0.096
6	8	0.171	0.188	0.212	9	0.095	0.096	0.092
7	6	0.102	0.155	0.181	12	0.095	0.095	0.082
8	4	0.003	0.135	0.152	8	0.096	0.096	0.093
9	13	0.123	0.133	0.193	6	0.095	0.073	0.093

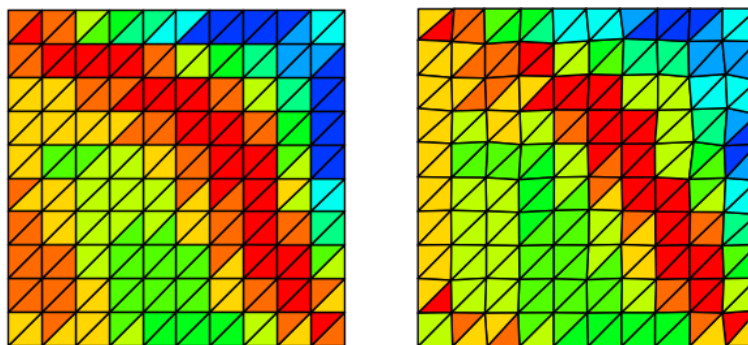


Figure 40: Plan of initial (left) and regularized (right) panels.

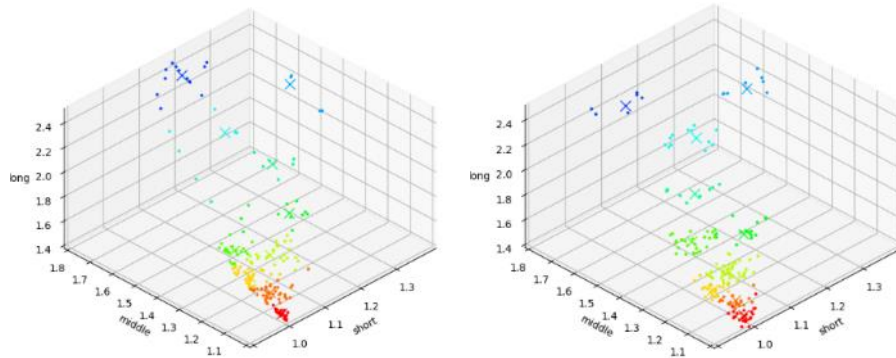


Figure 41: Clustering of edge lengths for initial (left) and regularized (right) solutions.

#### 4.2. Example 2: half-scaled surface

To inspect the relationship between pitch of the design surface and the outcome of regularization, our proposed method is applied to another surface, as shown in the Fig. 3, whose control polygon is the same as the last example in  $x$  and  $y$  coordinates and half in  $z$  coordinate. The number of mesh division, the connectivity of the nodes, and the domain of design variables  $\Omega_u$  and  $\Omega_v$  are also the same. Average lengths of long, middle, and short sides are 1.494, 1.058, and 1.014, respectively.

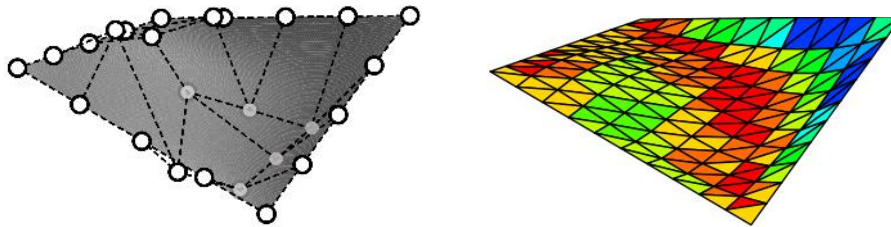


Figure 42: Control polygon of tensor product Bézier surface (left) and its initial panels (right).

After 100 iterations, the best regularized panelization is retrieved from 31st optimal solution and the result is described in Table 3. The largest difference of edge lengths for the initial panels is 0.067, on the other hand, it was reduced to 0.034 for the regularized ones. Since the curvature is smaller than the first example, the scale of objective value  $F$  in this example become smaller, accordingly.

Table 4: Regularization result.

cluster	Initial panelization			Regularized panelization				
	$N^i$	$L_i^U - L_i^L$	$L_m^U - L_m^L$	$L_s^U - L_s^L$	$N^i$	$L_i^U - L_i^L$	$L_m^U - L_m^L$	$L_s^U - L_s^L$
0	37	0.009	0.024	0.025	31	0.033	0.032	0.033
1	48	0.044	0.047	0.056	31	0.034	0.032	0.028
2	36	0.024	0.043	0.043	58	0.033	0.033	0.034
3	36	0.027	0.050	0.039	33	0.034	0.034	0.034
4	12	0.036	0.043	0.043	15	0.033	0.033	0.031
5	8	0.047	0.059	0.067	8	0.031	0.034	0.028
6	4	0.028	0.032	0.029	6	0.033	0.032	0.030
7	4	0.001	0.043	0.053	4	0.024	0.034	0.031
8	5	0.024	0.056	0.054	4	0.012	0.016	0.028
9	10	0.022	0.028	0.028	10	0.033	0.029	0.026

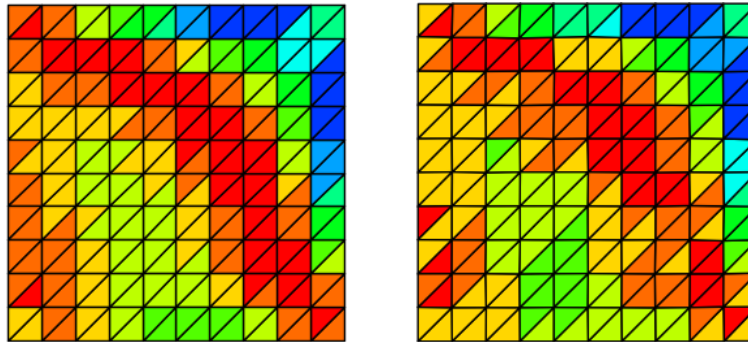


Figure 43: Plan of initial (left) and regularized (right) panels.

### 4.3. Structural analysis

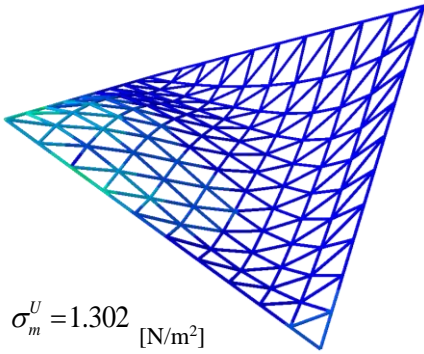
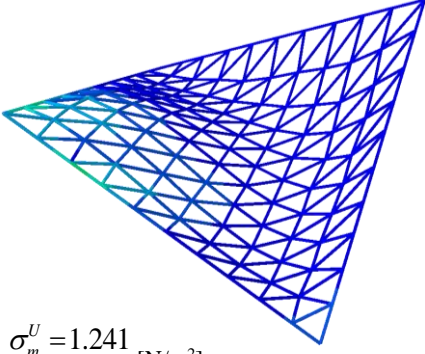
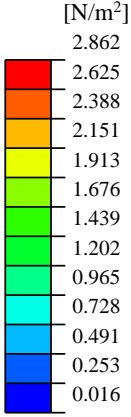
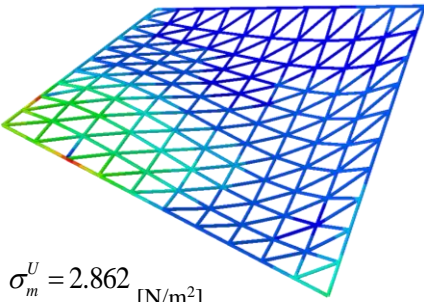
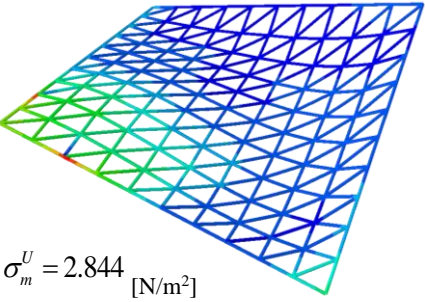
We compare structural performance of initial and optimal solutions under gravity load for the examples above. Panels are considered as non-structural elements; only beams connecting the triangular vertices are considered as structural members.

We use Abaqus 2016 to conduct the structural analysis. The members are circular pipes with a cross-section of outside diameter  $d = 0.05$  [m] and thickness  $t = 0.005$  [m], following the Timoshenko beam theory. Young's modulus is  $2.05 \times 10^{11}$  [N/m<sup>2</sup>], Poisson's ratio is 0.3, mass density is  $7870$  [kg/m<sup>3</sup>], and gravitational acceleration is  $9.8$  [N/kg].

Table 4 shows von Mises stresses of members with initial and regularized panelizations of the latticed shells in the previous subsections. The color-bar is unified among the four results; members colored in red are subject to large stress, and those in blue are to small stress.  $\sigma_m^U$  [N/m<sup>2</sup>] is the maximum value of von Mises stress of the members. The reduction of  $\sigma_m^U$  due to the regularization is negligibly small, because the initial solution already distributes member stresses relatively uniformly owing to the equal mesh division.

Considering the regularization results, it is observed that there is a trade-off between the degree of difficulty in regularization and member stresses in terms of the curvature of the design surface. In this case, by scaling the rise of the design surface by half, the measure of regularization  $F$  has reduced approximately by one-third; on the other hand, the maximum value of von Mises stress has increased to double.

Table 5: von Mises stresses of members.

	Initial solution	Regularized solution	Color
Ex. 1	 <p><math>\sigma_m^U = 1.302</math> [N/m<sup>2</sup>]</p>	 <p><math>\sigma_m^U = 1.241</math> [N/m<sup>2</sup>]</p>	<p>[N/m<sup>2</sup>]</p>  <p>2.862 2.625 2.388 2.151 1.913 1.676 1.439 1.202 0.965 0.728 0.491 0.253 0.016</p>
Ex. 2	 <p><math>\sigma_m^U = 2.862</math> [N/m<sup>2</sup>]</p>	 <p><math>\sigma_m^U = 2.844</math> [N/m<sup>2</sup>]</p>	

## 5. Conclusion

We proposed a regularization method of a triangular latticed shell designed on a tensor product Bézier surface. Continuous variables and Minkowski distance are introduced for degree of participation in the clustering process. In the optimization problem, difference of panel shapes are expressed also using Minkowski norm to preserve continuity of the objective function. By conducting clustering and optimization alternately and repeatedly, regularization result can improve especially in the early stage.

Furthermore, structural performances of initial and optimal solutions under gravity load are compared. We successfully quantify trade-off between construction cost represented by uniformness of panels and structural performance, by applying the degree of regularization (6) and von Mises stress to the evaluation, respectively.

## Acknowledgements

This work is supported by the “SPIRITS” program of Kyoto University and Grant-in-Aid for JSPS Research Fellow Grant Number 18J21456.

## References

- [1] M. Ohsaki and S. Fujita: Multiobjective shape optimization of latticed shells for elastic stiffness and uniform member lengths. Proc. Int. Symposium on Algorithmic Design for Architecture and Urban Design (ALGODE TOKYO 2011), 2011.

- [2] T. Ogawa, M. Ohsaki, R. Tateishi: Shape optimization of single-layer latticed shells for maximum linear buckling loads and uniform member lengths. *J. Struct. Constr. Eng., AIJ*, No. 570, 129-136, 2003.
- [3] Singh Mayank and Schaefer Scott: Triangle surfaces with discrete equivalence classes. *ACM Trans. Graph.* 29(4), 46, Proc. SIGGRAPH, 2010.
- [4] K. Hayashi and M. Ohsaki: Regularization of Triangular Lattice Shell Members and Panels for Bézier Surfaces. *Proc. Annual Symposium of International Association for Shell and Spatial Structures*, Boston, USA, Jul.16-20, Paper ID: 88, 2018.
- [5] D. Arthur. and S. Vassilvitskii: k-means++: the advantages of careful seeding. *Proceedings of the eighteenth annual ACM-SIAM symposium on Discrete algorithms*. Society for Industrial and Applied Mathematics Philadelphia, PA, USA. pp. 1027–1035, 2007.
- [6] A. Stetco, et al.: Fuzzy C-means++: Fuzzy C-means with effective seeding initialization, *Expert Systems with Applications*, Vol. 42(21), pp. 7541-7548, 2015.
- [7] D. Kraft: A software package for sequential quadratic programming. *Tech. Rep. DFVLR-FB 88-28*, DLR German Aerospace Center – Institute for Flight Mechanics, Koln, Germany. 1988.